Journal of Thermal Analysis and Calorimetry (2023) 148:13803–13814
https://doi.org/10.1007/s10973-023-12574-7

Preparation and characterization of surface-modified montmorillonite by cationic surfactants for adsorption purposes

Sara Arabmofrad[1] · Seid Mahdi Jafari[1] · Giuseppe Lazzara[2] · Aman Mohammad Ziaiifar[3] · Hoda Shahiri Tabarestani[1] · Ghasem Bahlakeh[3] · Giuseppe Cavallaro[2] · Martina Maria Calvino[2] · Mehdi Nasiri Sarvi[4]

Received: 30 March 2023 / Accepted: 18 September 2023 / Published online: 13 November 2023
© Akadémiai Kiadó, Budapest, Hungary 2023

Abstract

In this study, surface modification of montmorillonite with three types of cationic surfactants was investigated by adding different levels of surfactants corresponding to the CEC (cation exchange capacity) of montmorillonite; the surfactants were tetradecyl trimethylammonium bromide, cetyl trimethylammonium bromide, and didodecyl dimethylammonium bromide. Moreover, montmorillonite and modified montmorillonites were characterized by X-ray diffraction, Fourier transforms infrared spectroscopy, thermal analysis, contact angle, and zeta potential. Their surface morphologies were also determined by using the field emission scanning electron microscopy. The basal spacing of montmorillonite increased after intercalation of cationic surfactants, while the maximum basal spacing was influenced by increasing the molar mass of the surfactant. Also, for the same surfactant, maximum basal spacing enhanced when the CEC increased from 1:0 to 2:0. The results of Fourier transforms infrared spectroscopy indicated that intercalation of surfactants between montmorillonite layers leads to changes in functional groups of modified montmorillonite. To summarize, we successfully modified montmorillonite, making it a potential nanoadsorbent that could be used for the adsorption of valuable compounds such as phenolic compounds from wastewaters and byproducts of food industries.

Keywords Clay · Montmorillonite · Modification · Surfactants · Characterization · Morphology

Introduction

Nowadays, there is a growing interest toward the investigation of clay-based hybrid materials as they are promising in a wide range of applications from catalysis [1], environmental [2, 3], and cultural heritage preservation [4, 5].

Montmorillonite (Mt) which is a 2:1-type layered clay mineral characterized by propensity features such as high cation exchange capacity, large specific surface area, low cost, high swelling, and a porous structure is a perspective material in a wide variety of fields [6–8]. Mt can be applied in cosmetic [6, 6], environmental [9], and food industries [10]. The structure of Mt consists of an octahedral sheet (SiO_4) with four oxygen atoms in corners sandwiched by two tetrahedral sheets of Al_2O_3 with six oxygen in the corners [11, 12]. Due to the isomorphous substitution (e.g., Al^{3+}/Si^{4+} and Mg^{2+} or Fe^{2+}/Al^{3+} substitutions in the tetrahedral and octahedral), Mt has negative charges that are balanced by interlayer cations, e.g., Na^+, K^+, Ca^{2+}, Mg^{2+} [6, 13]. The interlayer cations can be exchanged with organic cations [14, 15].

Modified Mt (m-Mt), an artificially synthesized engineering material, is produced from raw Mt by using hydrophobic materials, such as cationic surfactants to enhance the properties of Mt for using in contaminant adsorption [6, 7, 16, 17]. Furthermore, cationic surfactants change the hydrophilic surface of Mt to hydrophobic conditions and cause high dispersion of Mt by interlayer space expansions [18, 19]. Different cationic surfactants have been used to synthesize m-Mt. These include no alkyl chain [20], low alkyl chain [6], long alkyl chain [9, 21], and single, double

✉ Seid Mahdi Jafari
smjafari@gau.ac.ir

1 Faculty of Food Science and Technology, Gorgan University of Agricultural Sciences and Natural Resources, Gorgan, Iran

2 Department of Physics and Chemistry, University of Palermo, Palermo, Italy

3 Department of Chemical Engineering, Golestan University, Aliabad Katoul, Iran

4 Department of Mining Engineering, Isfahan University of Technology, Isfahan, Iran

or triple alkyl chain surfactants [22, 23]. Among organic matters which are utilized in m-Mt, alkylammonium salts are well-known and preferred options [17]. The structure and characteristics of m-Mt depend on the type of surfactant and the original Mt used [24].

In this study, Mt was reacted with different cationic surfactants in terms of the alkyl chain lengths, namely, trimethyltetradecyl ammonium bromide (TTAB), cetyltrimethyl ammonium bromide (CTAB), and didodecyldimethyl ammonium bromide (DDAB). The amount of cationic surfactant in the interlayer space was 1 and 2 times the CEC (cation exchange capacity) of Mt for preparation of TTAB-Mt-x, CTAB-Mt-x, and DDAB-Mt-x ("x" = 1 and 2). The aim of this research was an increase in the adsorption capacity of Mt which leads to a synthesis of highly efficient adsorbent for applications in the food industry and separation of bioactive compounds such as phenolics from byproducts and wastewaters. For investigation of interlayer expansion and the interactions between Mt and alkylammonium ions, Mt and the resultant m-Mt were characterized using X-ray diffraction (XRD), Fourier transforms infrared (FT-IR) spectroscopy, as well as thermal analysis (TGA/DTG). Their surface morphologies were also investigated by field emission scanning electron microscopy (FESEM). Contact angle and zeta potential were also used to evaluate the hydrophilic-hydrophobic properties and surface charges of samples, respectively.

Materials and methods

The raw bentonite used in the present work was obtained from Salafchegan bentonite mine, Esfahan, Iran. CTAB was purchased from Merck, Germany, and the other surfactants including DDAB and TTAB were purchased from Fluka, Switzerland. Ammonium acetate (96%), sodium acetate (99%), and isopropyl alcohol were purchased from Merck, Germany. The properties of used surfactants in this study are provided in. Distilled water was used in all the experiments Table 1.

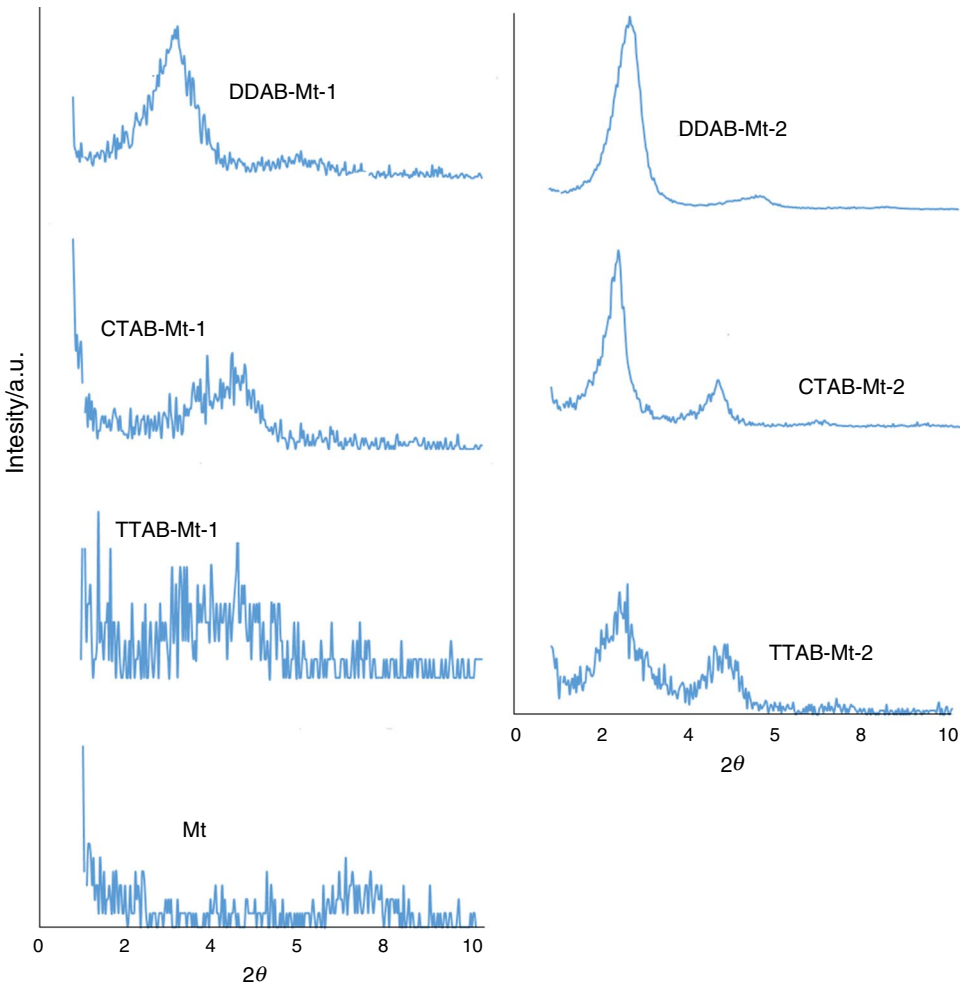

Fig. 1 XRD patterns of montmorillonite and modified montmorillonites

Table 1 The properties of used surfactants

Surfactant	Full name	Molecular formula	Structural formula	Weight molecular /g mol^{-1}	Impurities	CAS number
TTAB	Trimethyltetradecyl ammonium bromide	$C_{17}H_{38}BrN$	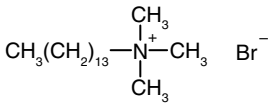	336.39	99%	1119–97-7
CTAB	Cetyltrimethyl ammonium bromide	$C_{19}H_{42}BrN$	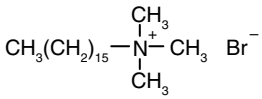	364.45	98%	57–09-0
DDAB	Didodecyldimethyl ammonium bromide	$C_{26}H_{56}BrN$	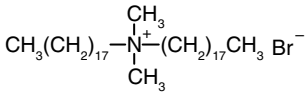	462.63	98%	3282–73-3

The chemical structure adapted with permission from https://www.tcichemicals.com/

Purification of bentonite

The purification of bentonite involved the following steps [25]: stirring bentonite (12 g) into distilled water (400 mL) at room temperature overnight by magnetic stirrer (Velp Scientifica ARE), then separation of the supernatant by centrifugation (Thermo Scientific Heraeus Multifuge 3S) at 1000 rpm for 4 min and drying at 110 °C in an oven (WTCbindco) for 24 h. After drying, purified Mt was obtained.

Determination of CEC

CEC is an important index showing the amount of exchangeable cations (Ca^{2+}, Mg^{2+}, K^{+}, and Na^{+}) that can neutralize negative charges on Mt surface [26]. The CEC of Mt after purification was 117 cmol(+)/kg, which was determined according to Chapman (1965).

Modification of Mt for production of m-Mts

The modification of Mt was performed according to Veiskarami et al. [25]. In order to perform this, purified Mt (4 g) from previous stage was dispersed in distilled water (400 mL), and the solution was stirred with a magnetic stirrer for 24 h at 80 °C so that Mt plates could be swelled; then surfactant solution (based on MMT 1.0 and 2.0 × CEC) was added to the Mt mixtures dropwise. After dropping, the resulting mixture was stirred overnight at room temperature. This process resulted in the insertion of surfactant chains into the interlayer spaces of Mt. The amount of surfactant added was according to the CEC of Mt. m-Mts were separated by centrifugation and washed with distilled water several times to remove excess salts. The obtained m-Mt was dried in an oven for 24 h at 110 °C.

Characterization of Mt and m-Mts

The XRD of samples were recorded on an XRD instrument (Asenware—AW-XDM300, China) using Cu with K-α1 = 1.54060 Å. The data were collected in the range of diffraction angle 0.5–10° (2θ) with a step size of 0.05° per second [27]. FT-IR spectra were performed on FT-IR spectrometer (Spectrum One, Perkin Elmer, Shelton, CT, USA) in the range of 400–4000 cm^{-1} at room temperature using the standard KBr pellets [28]. The FESEM images were obtained by a FESEM (Tescan-MIRAш, Czechia). Thermogravimetry/differential thermal analysis (TGA/DTG) was performed on a Q5000 IR apparatus (TA Instruments, New Castle, United States) between 25 and 700 °C at a rate of 10 °C min^{-1} under the nitrogen flow rate of 25 mL min^{-1} [28]. The contact angle of samples was obtained by an OCA 20 (Data Physics Instruments, Filderstadt, Germany) [6]. The zeta potential measurement of samples in suspensions at natural pH was performed using a Zetasizer instrument (Malvern Instruments, Malvern, UK) [29].

Results and discussion

The interlayer distance and scattering angle of Mt and m-Mts

The intercalation of surfactants into Mt was investigated through XRD, which gives information about basal spacing and the arrangement of sorbed surfactants in m-Mt layers. Figure 1 shows the small angle X-ray diffraction patterns

Table 2 XRD results of Mt and m-Mts

Sample	Position / °2θ	Basal spacing/ nm	Possible arrangement type in interlayer region
Mt	7.68	1.15	–
TTAB-Mt-1	4.51	1.95	Pseudo-trilayer
TTAB-Mt-2	2.43	3.61	Paraffin-type bilayer
CTAB-Mt-1	4.51	1.95	Pseudo-trilayer
CTAB-Mt-2	2.29	3.82	Paraffin-type bilayer
DDAB-Mt-1	3.11	2.83	Paraffin-type bilayer
DDAB-Mt-2	2.67	3.30	Paraffin-type bilayer

of both Mt and m-Mts. The typical XRD reflection band and *d*-value of MT were 2θ = 7.68 and 1.15 nm, respectively, which is identical to other studies; 1.48 nm [30], 1.16 nm [28]. As shown in Table 2, the basal reflection of Mt ($2\theta = 7.68°$) shifted to lower 2θ values (2.43–4.51°), and the basal spacing increased compared to Mt due to the surfactant intercalation. The distance of 1.95, 1.95, and 2.83 nm for TTAB-Mt-1, CTAB-Mt-1, and DDAB-Mt-1, respectively, indicates that surfactants with longer hydrophobic lengths had more benefits at expanding the interlayer space of Mt.

From Table 2, it can be concluded that the increase of CEC for all three surfactants from 1.0 to 2.0 was effective in expanding the interlayer space of Mt; intercalation of TTAB, CTAB, and DDAB increased the basal spacing from 1.95, 1.95, and 2.84 to 3.61, 3.82, and 3.31 nm, respectively. It is similar to the results in the literature about modification of Mt with cationic surfactants: CTAB, TTAB, tetrabutylammonium bromide, dodecyl trimethylammonium bromide, decyl trimethylammonium bromide, octyl trimethylammonium bromide [6], CTAB, tetramethylammonium bromide (TMA) [18], and DDAB [31]. Similar to our findings, they reported that the basal spacing of Mt increased from 1.23 nm to 1.76 nm with rise in the alkyl chain length from 8 to 16. Also, the adsorption level of surfactants onto Mt surface is correlated with surfactant loading. In contrast, there were no changes in the basal spacing of Mt modified with short alkyl chain (TMA) according to different CEC (0.5, 1, and 1.5), compared to Mt.

Based on previous studies, there is a correlation between length and height of a surfactant, and basal spacing as well as surfactant concentration which correspondingly affect the alkyl chain arrangements [21]. According to some researches [32, 33], the heights of TTAB and CTAB are 0.4 or 0.45 nm based on their orientation and their length are 1.58 and 2.14 nm, respectively. The interlayer spacing of TTAB-Mt-1 and CTAB-Mt-1 was 1.95 nm suggesting that there are parallel alkyl chains into Mt layers, forming pseudo-trilayer structures. Also, basal spacing of TTAB-Mt-2 and CTAB-Mt-2 that were 3.61 and 3.82 reveals that with the increase in layer spacing and surfactant loading, the structure of TTAB-Mt-2 and CTAB-Mt-2 became probably paraffin-type bilayers. DDAB-Mt-1 and DDAB-Mt-2 probably have paraffin-type bilayer structures close to values observed by Flores et al. [22], Lazorenko et al. [34], and Sun et al. [31].

Functional groups of the surface of Mt and m-Mts

FT-IR technique is used to probe the confirmations of the structural changes in Mt after intercalation of surfactant into Mt. Moreover, representative FT-IR spectra of Mt and m-Mts are presented in Fig. 2. Two bands are at 521 cm^{-1} and 465 cm^{-1} owing to layered Al–O–Si and Si–O-Si bending vibration, while that at 1040 cm^{-1} and 1641 cm^{-1} are attributed to the Si–O stretching vibration and OH bending vibration, respectively [35, 36]. The bands at 3629 cm^{-1} correspond to the O–H stretching vibration of Al–OH and Si–OH groups Mt [37, 38]. The presence of bonds 2920 cm^{-1} and 2850 cm^{-1} corresponding to C-H stretching of CH_2 and CH_3 alkyl chain of surfactant can confirm the intercalation of surfactant ions into the interlayers of Mt or adsorption on the surface of Mt, as well as a band around 1470 cm^{-1} which corresponds to the C–H bending in methyl and methylene groups [36, 39]. The results of XRD and FT-IR indicated that the surfactant ions were present in Mt. The main adsorption bands are summarized in Table 3.

The morphology of Mt and m-Mts

FESEM analysis was carried out to evaluate surface morphologies of Mt and m-Mts and the images with various magnifications are given in Fig. 3. FESEM imaging showed that Mt had a typical lamellar and heterogeneous, aggregated, and bulky morphology. Mt had fine particles with non-uniform size distribution [6]. From the FESEM images of m-Mts, it was observed larger structures with uniform size distribution due to surfactant ions insertion into the layer and agglomeration of m-Mt particles resulted in the removal of electrostatic repulsive forces with modification as confirmed by zeta potential and XRD results [17, 40, 41]. Similarly, Abolhasani et al. [42] and Widjonarko et al. [43] reported that when cationic surfactant ions were absorbed into the interlayer space, they not only expanded the interlayer spacing, but also Mt with bulky shape changed to larger particles with a porous surface.

The thermal properties of Mt and m-Mts

TGA is an essential technique for studying the general thermal behavior of Mt and m-Mts at certain temperatures [44–46]. Figure 4 reports the changes in the sample mass (TGA) and the rate of changes in the mass (DTG) with the

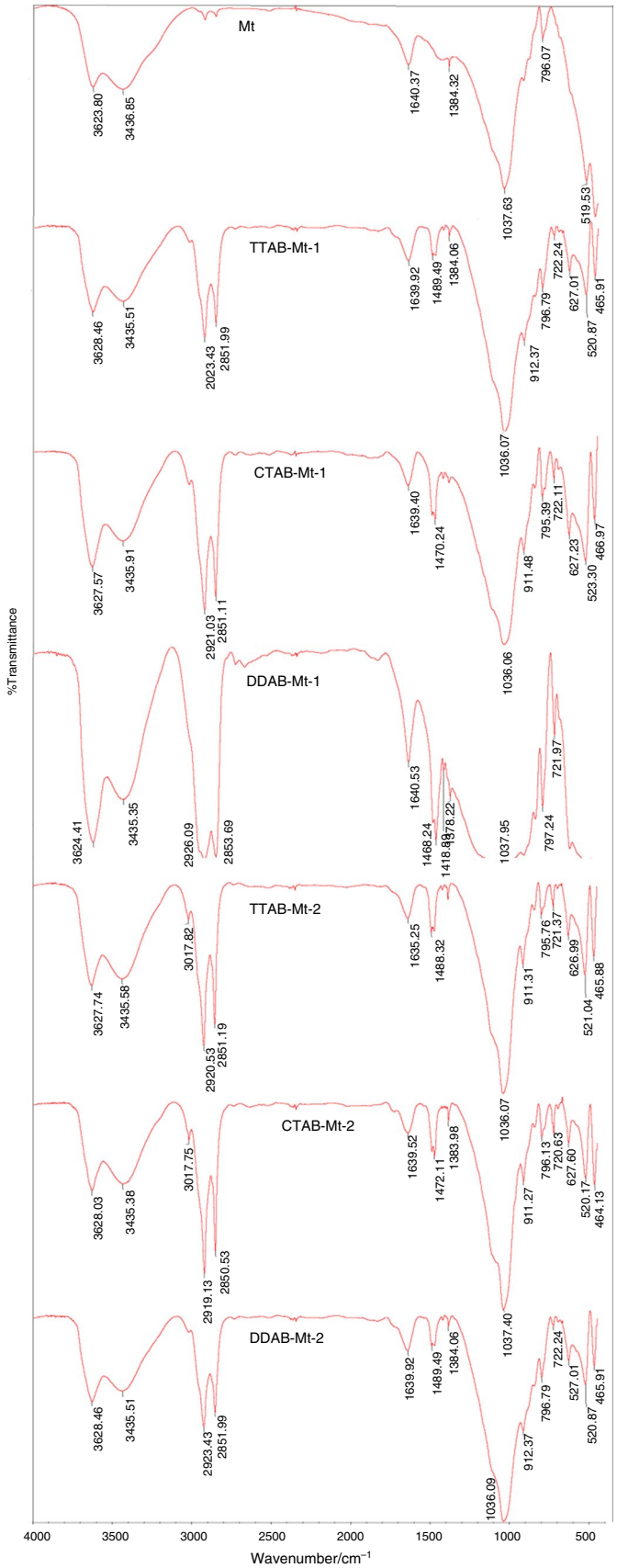

Fig. 2 FT-IR spectra of Mt and m-Mts

Table 3 Positions and assignments of FT-IR vibration bands in raw Mt and m-Mts

Assignment	Wavenumber/cm^{-1}						
	Mt	CTAB-Mt-1	CTAB-Mt-2	TTAB-Mt-1	TTAB-Mt-2	DDAB-Mt-1	DDAB-Mt-2
Al–O–Si stretching	520	523	520	520	521	524	520
CH_2 rocking	796	795	796	797	796	797	796
Si–O stretching	1037	1036	1037	1036	1036	1037	1036
H–O–H bending (ν2)	1639	1639	1639	1640	1639	1641	1642
Structural OH stretching	3627	3627	3628	3628	3628	3624	3625
CH_2 scissoring	–	1470	1472	1489	1488	1468	1468
Symmetric CH_2 stretching	–	2851	2850	2852	2851	2853	2853
Asymmetric CH_2 stretching	–	2921	2919	2923	2920	2926	2924

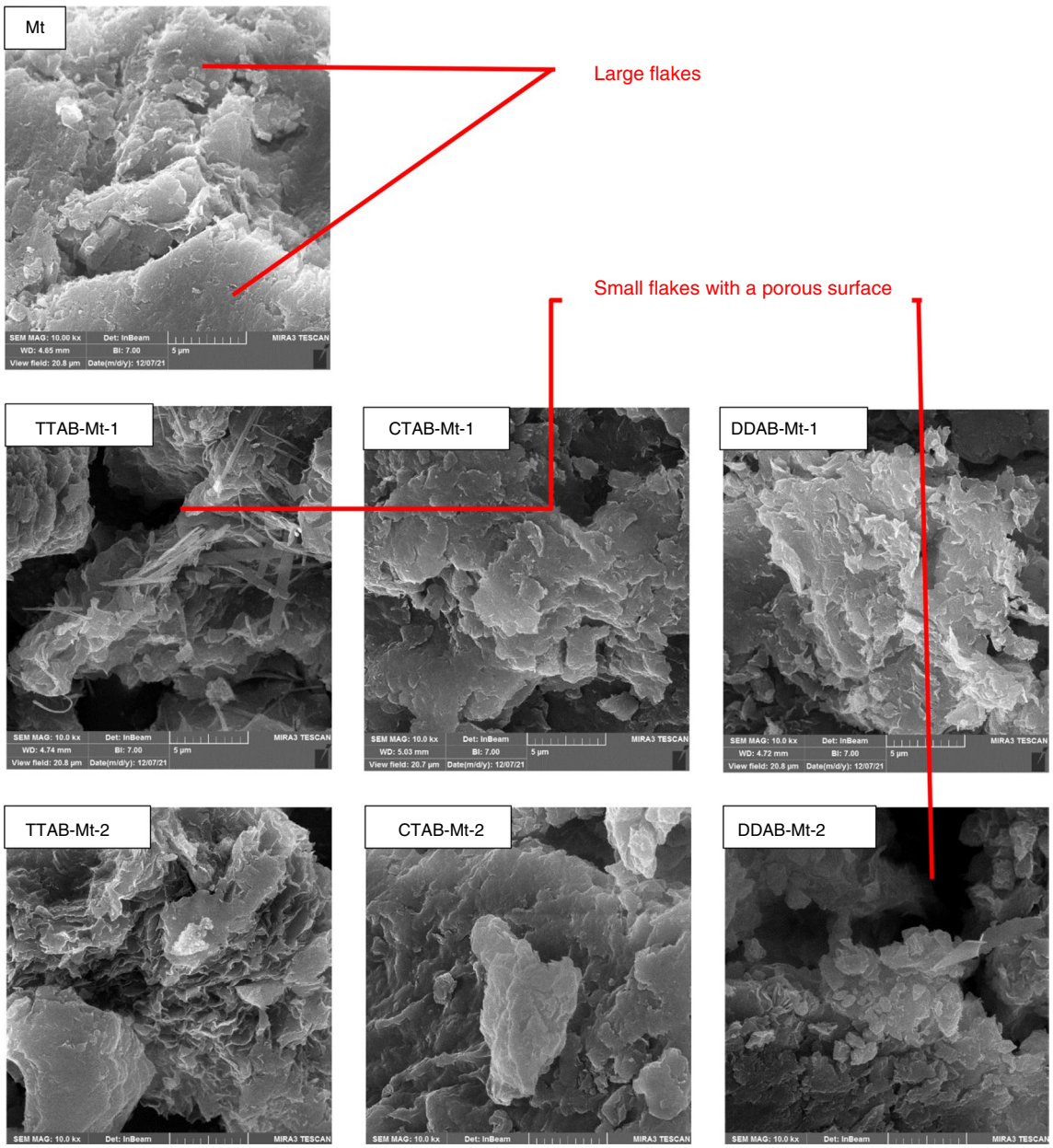

Fig. 3 FESEM micrographs of Mt and m-Mts

temperature for Mt and m-Mts. In Table 4, TGA results are displayed and they indicated that there were several step mass losses in the decomposition process of Mt and m-Mts during the heating: the mass loss of adsorbed water for all samples at ca. 70 °C [47]; finally, the significant mass loss at 214–309 °C due to the decomposition of the cationic surfactants and the dehydroxylation of Mt for temperatures above 530 °C [28]. The differences between the water content of Mt and m-Mt is related to the intercalation of surfactants into Mt [28] that generated a water displacement. Decomposition temperature of pure cationic surfactants (DDAB: 214.49 °C, CTAB:260.11 °C, and TTAB: 275.75 °C) was moved toward larger temperatures for m-Mts (218.17- 308.95 °C) because of the interaction with Mt that hinders mass transport and thermally stabilize the surfactant moiety.As evident from DTG curves, the peak of m-Mts between 200 and 400 °C corresponding to surfactant molecules in m-Mts with CEC = 2.0 was much higher than m-Mts with CEC = 1.0 due to the presence of a large number of surfactants in m-Mt [28]. On the other side, the maximum mass loss rate temperature of the m-Mt increased with decreasing the length of the alkyl chain of surfactant and CEC (TTAB-Mt-1 > TTAB-Mt-2 > CTAB-Mt-1 > CTAB-Mt-2 > DDAB-Mt-1 > DDAB-Mt-2). Supposedly, higher decomposition temperature is related to the stronger interactions between cationic surfactants and Mt and arrangement type of cationic surfactants in interlayer region due to changes of required decomposition energy [48, 49].

The hydrophilicity/hydrophobicity of Mt and m-Mts

The contact angle was used for checking the hydrophilicity/hydrophobicity of samples determined by placing a drop of water on their surface. The values of contact angles are shown in Fig. 5. These findings helped us to investigate the interaction between Mt and cationic surfactant in two levels. The hydrophilicity of Mt, which is affected by the diffusion of water molecules into the interlayer space of Mt and the presence of hydrophilic ions and groups, causes a small contact angle (30.65°) as described previously [50]. However, with the addition of surfactants, due to the hydrophobicity of the surfactant chains, the hydrophilicity of m-Mts was decreased, and therefore, the contact angles of m-Mts were larger than that for Mt. It was observed that the contact angle of CEC = 2.0 equivalent surfactants were lower than that at CEC = 1.0 equivalent surfactants (CTAB-Mt-1: 67.20 > CTAB-Mt-2:55.45, TTAB-Mt-1: 66.40° > TTAB-Mt-2: 51.90°, DDAB-Mt-1:69.10° > DDAB-Mt-2: 67.40°). This situation has pointed to form the paraffinic bilayer structure. Due to the repulsion between similar charges of the hydrophobic tail of the surfactants, this formation leads to partial interlayer expansion [50]. Furthermore, the contact angle was increased by increasing the hydrophobic alkyl chain length and number of alkyl chains (DDAB-Mt with two alkyl chains > CTAB-Mt > TTAB-Mt), which indicates that m-Mt became more hydrophobic [6, 51]. These results are in agreement with the data obtained from zeta potential (Sect. Surface charge of Mt and m-Mts).

Surface charge of Mt and m-Mts

For investigation of the surface characteristic of samples, surface charges of Mt and m-Mts were measured using zeta potential. Mt had a negative zeta potential = −21.6 mV which was similar to results (−31 ± 1 mV) from Kumar et al. (2020). The negative charge of Mt is related to the isomorphic substitution of Fe^{2+} and Mg^{2+} ions for Al^{3+} in the octahedral sites and Al^{3+} for Si^{+4} in the tetrahedral sites [35, 52, 53]. With the addition of surfactants to Mt, the surface charge tends to be positive. It was seen that CEC = 1.0 equivalent TTAB cannot completely neutralize the negative charge on the Mt surface (−2.54 mV), whereas CTAB-Mt-1 and DDAB-Mt-1 had positive surface charges (+4.63 and 13.36 mV, respectively) [29, 54]. In addition, the negative value of zeta potential for TTAB-Mt-1 and positive value of zeta potential for other m-Mts may imply that the ion exchange and electrostatic interactions were more effective, respectively, in the adsorption of surfactants [6].

The results of zeta potentials (Fig. 6) show that the surface charge of m-Mts increased as the CEC ratio increased. However, the zeta potential and positively change of TTAB-Mt-2 and CTAB-Mt-2 (18.4 and 13.56) were > TTAB-Mt-1, CTAB-Mt-1 (−2.45 and 4.63 mV, respectively) due to the adsorption of more surfactants on the external surface of Mt [22, 55, 56]. This situation is related to the transformation of some surfactant ions in Mt layers from the pseudo-trilayer structures to the paraffinic bilayer structure. The decrease in contact angle and XRD observations (Table 2) supports this result. On the other side, the zeta potential of m-Mt increased at higher length of surfactants (DDAB-Mt > CTAB-Mt > TTAB-Mt) since Mt modified with longer length surfactants can be expected to be more hydrophobic. The finding of zeta potential was supported by contact angle measurements. The results of [6, 6] who used six cationic surfactants with different chain lengths (C_{16}, C_{14}, C_{12}, $C_{10,}$ and C_8) for modification of Mt revealed the adsorption of the surfactants on Mt surface increased as confirmed with zeta potential data.

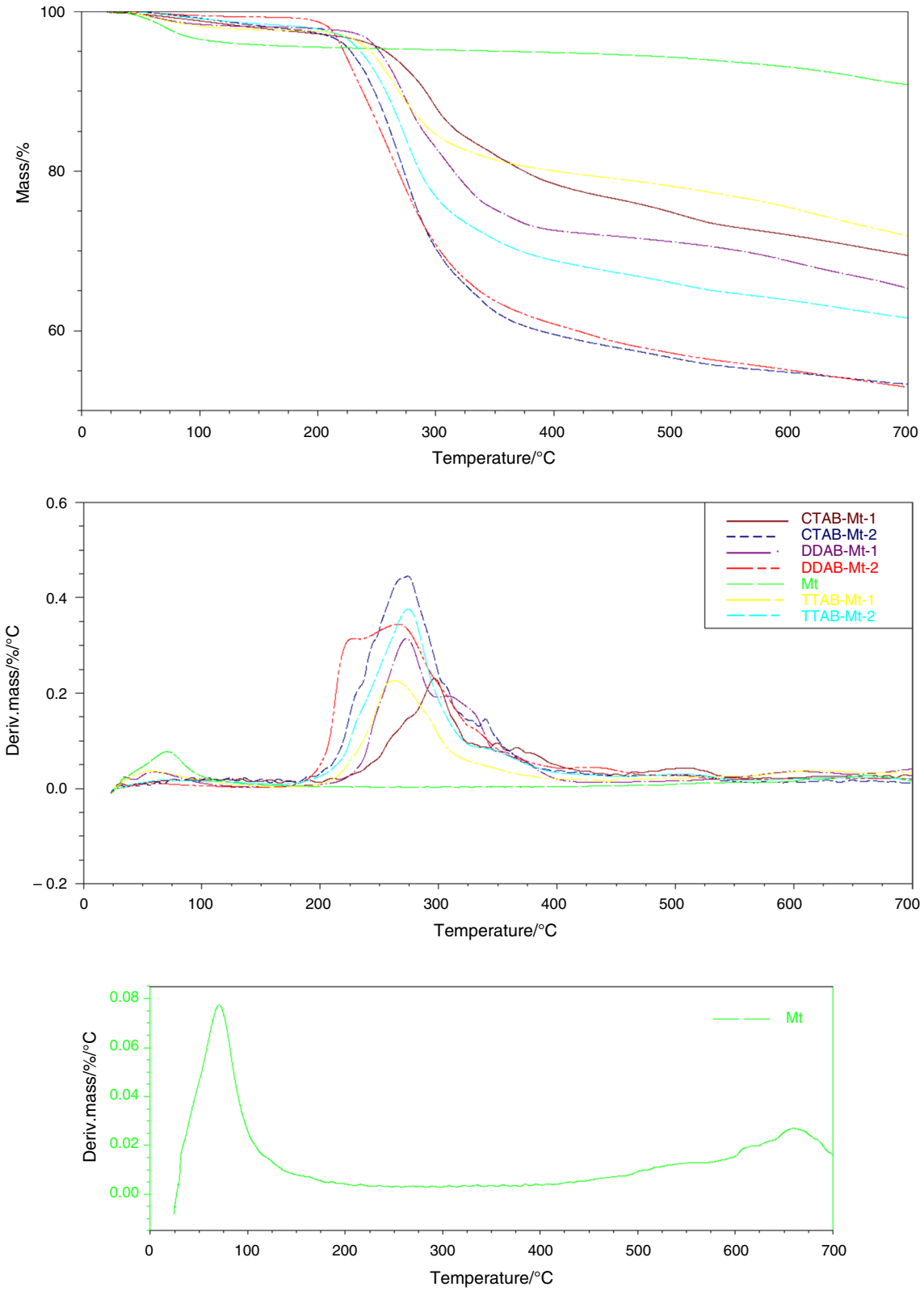

Fig. 4 TGA and derivative curves of Mt and m-Mts

Table 4 TGA results of Mt and m-Mts

Sample	Mass loss/%	Step one dehydration (Temp /°C)	Step three de-surfactant (Temp /°C)	Step four dehydroxylation (Temp /°C)
Mt	9.05	75.37	–	638.40
TTAB-Mt-1	28.21	77.68	308.95	–
TTAB-Mt-2	38.43	66.13	304.96	548.20
TTAB	99.72	–	275.75	–
CTAB-Mt-1	30.42	76.52	276.30	536.91
CTAB-Mt-2	46.77	74.36	264.99	537.66
CTAB	99.92	–	260.11	–
DDAB-Mt-1	34.69	75.11	260.35	578.32
DDAB-Mt-2	47.07	76.84	218.17	529.50
DDAB	99.55	–	214.49	–

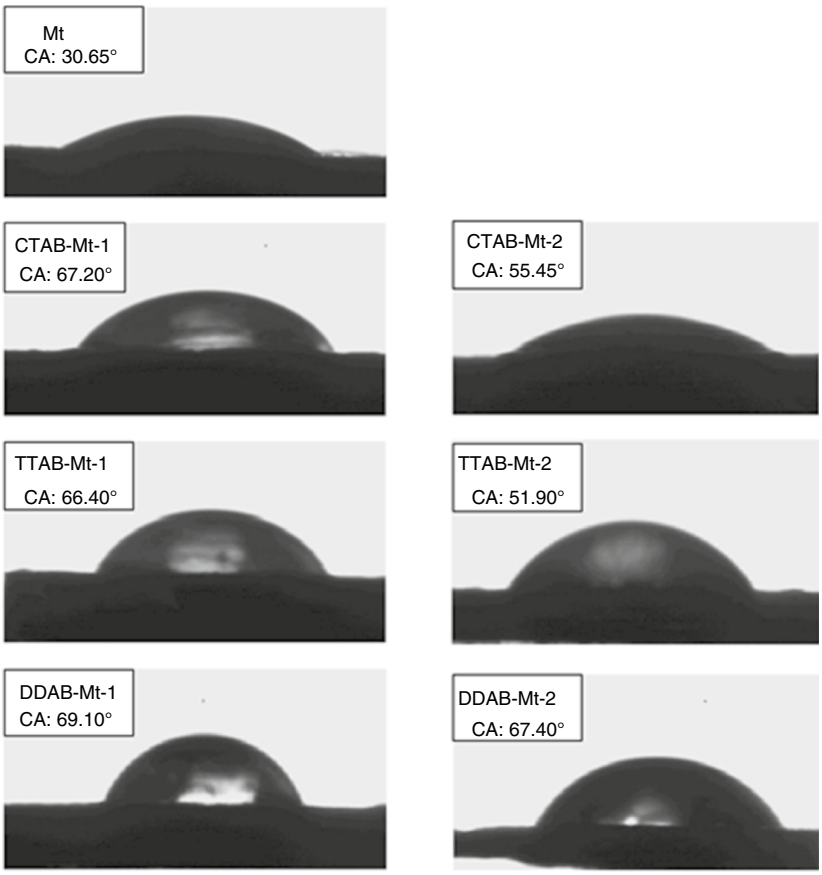

Fig. 5 Contact angle (CA) of Mt and m-Mts

Conclusions

In this study, we modified Mt using cationic surfactants with different alkyl chain lengths. The results of XRD confirmed that modification of Mt with all three cationic surfactants was done successfully, and the basal spacing increased at higher alkyl chain lengths, and CEC correspondingly affected the alkyl chain arrangements. From FT-IR spectra of samples, the incorporation of three types of surfactant ions in the Mt layer and the change of hydrophilicity of Mt after modification was approved. FESEM images revealed agglomeration of m-Mt particles after modification. Zeta potential and contact angle data, respectively, showed the surface of Mt to be hydrophilic, and the zeta potential shifted to a positive value after intercalation of surfactant ions; also both values increased at higher length of surfactants. The loaded cationic

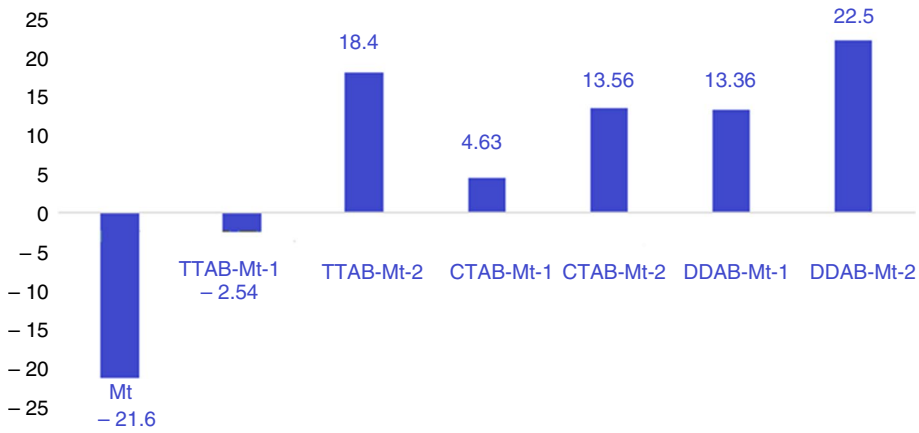

Fig. 6 The zeta potential of Mt and m-Mts

surfactants were studied by TGA/DTG analysis that identified four mass loss steps as a result of water desorption, dehydration, surfactant decomposition, and dehydroxylation. These m-Mt s have the potential for recovery of valuable compounds from wastewater such as phenolic compounds or removal of environmental pollutants such as phenol, dyes, and heavy metals.

Acknowledgements We are grateful to Iranian National Science Foundation (INSF) for the financial Support (97006593). We also thank Gorgan University of Agricultural Sciences and Natural Resources and University of Palermo (Department of Physics and Chemistry) for their supports.

Author contribution SA contributed to formal analysis, methodology, data curation, writing, original draft preparation, software, and review and editing. SMJ helped in supervision, project administration, funding acquisition, and review and editing. GL contributed to data curation, formal analysis, validation funding acquisition, and review and editing. AMZ, HST, and GB helped in investigation. GC contributed to data curation. MMC and MNS helped in methodology and validation.

Data availability Data for this study are available inside the manuscript.

Declarations

Conflict of interests The authors declare no competing interests.

Ethical approval Not applicable.

Consent to participate All the authors of this work agree with the content and give their explicit consent to submit it.

Consent for publish All the authors agree for consent for the publication, and the current article does not contain data from any individual person.

References

1. Lisuzzo L, Cavallaro G, Milioto S, Lazzara G. Halloysite nanotubes as nanoreactors for heterogeneous micellar catalysis. J Colloid Interface Sci. 2022;608:424–34. https://doi.org/10.1016/j.jcis.2021.09.146.
2. Cavallaro G, Lazzara G, Rozhina E, et al. Organic-nanoclay composite materials as removal agents for environmental decontamination. RSC Adv. 2019;9:40553–64. https://doi.org/10.1039/C9RA08230A.
3. Ewis D, Ba-Abbad MM, Benamor A, El-Naas MH. Adsorption of organic water pollutants by clays and clay minerals composites: a comprehensive review. Appl Clay Sci. 2022;229: 106686. https://doi.org/10.1016/j.clay.2022.106686.
4. Cavallaro G, Milioto S, Lazzara G. Halloysite nanotubes: interfacial properties and applications in cultural heritage. Langmuir. 2020;36:3677–89. https://doi.org/10.1021/acs.langmuir.0c00573.
5. Lisuzzo L, Hueckel T, Cavallaro G, et al. Pickering emulsions based on wax and halloysite nanotubes: an ecofriendly protocol for the treatment of archeological woods. ACS Appl Mater Interfaces. 2021;13:1651–61. https://doi.org/10.1021/acsami.0c20443.
6. Açışlı Ö, Karaca S, Gürses A. Investigation of the alkyl chain lengths of surfactants on their adsorption by montmorillonite (Mt) from aqueous solutions. Appl Clay Sci. 2017;142:90–9.
7. Ma L, Chen Q, Zhu J, et al. Adsorption of phenol and Cu (II) onto cationic and zwitterionic surfactant modified montmorillonite in single and binary systems. Chem Eng J. 2016;283:880–8.
8. Zhu R, Chen Q, Zhou Q, et al. Adsorbents based on montmorillonite for contaminant removal from water: a review. Appl Clay Sci. 2016;123:239–58.
9. Liao L, Lv G, Cai D, Wu L. The sequential intercalation of three types of surfactants into sodium montmorillonite. Appl Clay Sci. 2016;119:82–6.
10. Ruankaew N, Kristinawati A, Yoshida N, Phongphanphanee S. A 3D-RISM study of water and potassium ion adsorption in montmorillonite nanoclay. IOP Conf Ser Mater Sci Eng. 2020;773:012060. https://doi.org/10.1088/1757-899X/773/1/012060.
11. Jiraskova Y, Bursik J, Seidlerova J, et al. Microstructural analysis and magnetic characterization of native and magnetically modified montmorillonite and vermiculite. J Nanomater. 2018;2018:e3738106. https://doi.org/10.1155/2018/3738106.
12. Kumari N, Mohan C. Basics of clay minerals and their characteristic properties. Clay Clay Miner Work Title. 2021. https://doi.org/10.5772/intechopen.97672.
13. Morata A, Loira I (2016) Grape and Wine Biotechnology. BoD – Books on Demand
14. Fu M, Zhang Z, Wu L, et al. Investigation on the co-modification process of montmorillonite by anionic and cationic surfactants. Appl Clay Sci. 2016;132:694–701.
15. Kim D-G, Song D-I, Jeon Y-W. pH-dependent sorptions of phenolic compounds onto montmorillonite modified with

hexadecyltrimethylammonium cation. Sep Sci Technol. 2001;36:3159–74.
16. Sciascia L, Casella S, Cavallaro G, et al. Olive mill wastewaters decontamination based on organo-nano-clay composites. Ceram Int. 2019;45:2751–9. https://doi.org/10.1016/j.ceramint.2018.08.155.
17. Zhao Q, Choo H, Bhatt A, et al. Review of the fundamental geochemical and physical behaviors of organoclays in barrier applications. Appl Clay Sci. 2017;142:2–20. https://doi.org/10.1016/j.clay.2016.11.024.
18. Abbas A, Sallam AS, Usman AR, Al-Wabel MI. Organoclay-based nanoparticles from montmorillonite and natural clay deposits: Synthesis, characteristics, and application for MTBE removal. Appl Clay Sci. 2017;142:21–9.
19. Boyd SA, Shaobai S, Lee J-F, Mortland MM. Pentachlorophenol Sorption by Organo-Clays. Clays Clay Miner. 1988;36:125–30. https://doi.org/10.1346/CCMN.1988.0360204.
20. Deng L, Liu Y, Zhuang G, et al. Dynamic benzene adsorption performance of microporous TMA+-exchanged montmorillonite: The role of TMA+ cations. Microporous Mesoporous Mater. 2020;296: 109994. https://doi.org/10.1016/j.micromeso.2019.109994.
21. Hu Z, He G, Liu Y, et al. Effects of surfactant concentration on alkyl chain arrangements in dry and swollen organic montmorillonite. Appl Clay Sci. 2013;75–76:134–40. https://doi.org/10.1016/j.clay.2013.03.004.
22. Flores FM, Undabeytia T, Jaworski M, et al. Organo-montmorillonites as adsorbent materials for thiophanate-methyl removal: Adsorption-desorption studies and technological applications. J Environ Chem Eng. 2020;8: 103806. https://doi.org/10.1016/j.jece.2020.103806.
23. Yang Q, Gao M, Zang W. Comparative study of 2,4,6-trichlorophenol adsorption by montmorillonites functionalized with surfactants differing in the number of head group and alkyl chain. Colloids Surf Physicochem Eng Asp. 2017;520:805–16. https://doi.org/10.1016/j.colsurfa.2017.02.057.
24. He H, Ma Y, Zhu J, et al. Organoclays prepared from montmorillonites with different cation exchange capacity and surfactant configuration. Appl Clay Sci. 2010;48(1–2):67–72.
25. Veiskarami M, Sarvi MN, Mokhtari AR. Influence of the purity of montmorillonite on its surface modification with an alkyl-ammonium salt. Appl Clay Sci. 2016;120:111–20. https://doi.org/10.1016/j.clay.2015.10.026.
26. Durães N, Novo LAB, Candeias C, da Silva EF. Chapter 2 - Distribution, Transport and Fate of Pollutants. In: Duarte AC, Cachada A, Rocha-Santos T, editors. Soil Pollution. Academic Press; 2018. p. 29–57.
27. Aliabadi M, Dastjerdi R, Kabiri K. HTCC-modified nanoclay for tissue engineering applications: a synergistic cell growth and antibacterial efficiency. BioMed Res Int. 2013;2013: 749240. https://doi.org/10.1155/2013/749240.
28. Muñoz-Shugulí C, Rodríguez FJ, Bruna JE, et al. Cetylpyridinium bromide-modified montmorillonite as filler in low density polyethylene nanocomposite films. Appl Clay Sci. 2019;168:203–10.
29. Luo W, Sasaki K, Hirajima T. Surfactant-modified montmorillonite by benzyloctadecyldimethylammonium chloride for removal of perchlorate. Colloids Surf Physicochem Eng Asp. 2015;481:616–25. https://doi.org/10.1016/j.colsurfa.2015.06.025.
30. Choi J, Shin WS. Removal of salicylic and ibuprofen by hexadecyltrimethylammonium-modified montmorillonite and zeolite. Minerals. 2020;10:898. https://doi.org/10.3390/min10100898.
31. Sun Z, Park Y, Zheng S, et al. XRD, TEM, and thermal analysis of Arizona Ca-montmorillonites modified with didodecyldimethylammonium bromide. J Colloid Interface Sci. 2013;408:75–81. https://doi.org/10.1016/j.jcis.2013.07.007.
32. Chanra J, Budianto E, Soegijono B (2019), Surface modification of montmorillonite by the use of organic cations via conventional ion exchange method. In: IOP Conference Series: Materials Science and Engineering. IOP Publishing; 012057
33. Ltifi I, Ayari F, Chehimi DBH, Ayadi MT. Physicochemical characteristics of organophilic clays prepared using two organo-modifiers: alkylammonium cation arrangement models. Appl Water Sci. 2018;8:91. https://doi.org/10.1007/s13201-018-0732-8.
34. Lazorenko G, Kasprzhitskii A, Yavna V. Comparative study of the hydrophobicity of organo-montmorillonite modified with cationic. Amphot Nonionic Surf Min. 2020;10:732. https://doi.org/10.3390/min10090732.
35. Dos Santos A, Viante MF, Pochapski DJ, et al. Enhanced removal of p-nitrophenol from aqueous media by montmorillonite clay modified with a cationic surfactant. J Hazard Mater. 2018;355:136–44.
36. Moslemizadeh A, Khezerloo-ye Aghdam S, Shahbazi K, et al. Assessment of swelling inhibitive effect of CTAB adsorption on montmorillonite in aqueous phase. Appl Clay Sci. 2016;127–128:111–22. https://doi.org/10.1016/j.clay.2016.04.014.
37. Caccamo MT, Mavilia G, Mavilia L, et al. Self-assembly processes in hydrated montmorillonite by FTIR investigations. Materials. 2020;13:1100. https://doi.org/10.3390/ma13051100.
38. Edraki M, Zaarei D. Modification of montmorillonite clay with 2-mercaptobenzimidazole and investigation of their antimicrobial properties. Asian J Green Chem. 2018;2:189–200. https://doi.org/10.22034/ajgc.2018.58088.
39. Obradović M, Daković A, Smiljanić D, et al. Ibuprofen and diclofenac sodium adsorption onto functionalized minerals: Equilibrium, kinetic and thermodynamic studies. Microporous Mesoporous Mater. 2022;335: 111795. https://doi.org/10.1016/j.micromeso.2022.111795.
40. Kıranşan M, Soltani RDC, Hassani A, et al. Preparation of cetyltrimethylammonium bromide modified montmorillonite nanomaterial for adsorption of a textile dye. J Taiwan Inst Chem Eng. 2014;45:2565–77.
41. Praus P, Turicová M, Študentová S, Ritz M. Study of cetyltrimethylammonium and cetylpyridinium adsorption on montmorillonite. J Colloid Interface Sci. 2006;304:29–36. https://doi.org/10.1016/j.jcis.2006.08.038.
42. Abolhasani M, Lakzian A, Fotovat A, Khorasani R. Synthesis of organo-montmorillonite and its effect on soil urease and L-glutaminase activites. Eurasian Soil Sci. 2017;50:613–9.
43. Widjonarko DM, Mayasari OD, Wahyuningsih S, Nugrahaningtyas KD. Modification of Montmorillonite with Cetyl Trimethylammonium Bromide and Tetra Ethyl Ortho Silicate. IOP Conf Ser Mater Sci Eng. 2018;333: 012048. https://doi.org/10.1088/1757-899X/333/1/012048.
44. Calabrese I, Cavallaro G, Lazzara G, et al. Preparation and characterization of bio-organoclays using nonionic surfactant. Adsorption. 2016;22:105–16.
45. Cavallaro G, Lazzara G, Milioto S, et al. Modified halloysite nanotubes: nanoarchitectures for enhancing the capture of oils from vapor and liquid phases. ACS Appl Mater Interfaces. 2014;6:606–12.
46. del Hoyo C, Dorado C, Rodríguez-Cruz MS, Sánchez-Martín MJ. Physico-chemical study of selected surfactant-clay mineral systems. J Therm Anal Calorim. 2008;94:227–34. https://doi.org/10.1007/s10973-007-8934-6.
47. Zhu J, Shen W, Ma Y, et al. The influence of alkyl chain length on surfactant distribution within organo-montmorillonites and their thermal stability. J Therm Anal Calorim. 2012;109:301–9.
48. Cesniene J, Baltušnikas A, Brinkienė K (2014) Modification and characterization of MBDHTA + intercalated nanoclay. https://www.semanticscholar.org/paper/Modification-and-characteri

zation-of-MBDHTA-%2B-Cesniene-Baltu%C5%A1nikas/e578b8ac647ccd0d9c73b55ddea493699e419975. Accessed 11 Aug 2022
49. Ouellet-Plamondoncm CM, Stasiak J, Al-Tabbaa A. The effect of cationic, non-ionic and amphiphilic surfactants on the intercalation of bentonite. Colloids Surf Physicochem Eng Asp. 2014;444:330–7. https://doi.org/10.1016/j.colsurfa.2013.12.032.
50. Karaca S, Gürses A, Ejder Korucu M. Investigation of the Orientation of C T A + Ions in the Interlayer of CTAB Pillared Montmorillonite. J Chem. 2012;2013: e274838. https://doi.org/10.1155/2013/274838.
51. Ren H-P, Tian S-P, Zhu M, et al. Modification of montmorillonite by Gemini surfactants with different chain lengths and its adsorption behavior for methyl orange. Appl Clay Sci. 2018;151:29–36. https://doi.org/10.1016/j.clay.2017.10.024.
52. Chatterjee A, Iwasaki T, Ebina T, Hayashi H. Relationship between infrared spectra and isomorphous substitution in smectites: a computer simulation study. J Mol Graph. 1996;14(302–305):285–6. https://doi.org/10.1016/s0263-7855(96)00083-5.
53. Shah KJ, Mishra MK, Shukla AD, et al. Controlling wettability and hydrophobicity of organoclays modified with quaternary ammonium surfactants. J Colloid Interface Sci. 2013;407:493–9.
54. Zhang L, Zhang B, Wu T, et al. Adsorption behavior and mechanism of chlorophenols onto organoclays in aqueous solution. Colloids Surf Physicochem Eng Asp. 2015;484:118–29. https://doi.org/10.1016/j.colsurfa.2015.07.055.
55. Bianchi AE, Fernández M, Pantanetti M, et al. ODTMA+ and HDTMA+ organo-montmorillonites characterization: new insight by WAXS, SAXS and surface charge. Appl Clay Sci. 2013;83–84:280–5. https://doi.org/10.1016/j.clay.2013.08.032.
56. Thomas F, Michot LJ, Vantelon D, et al. Layer charge and electrophoretic mobility of smectites. Colloids Surf Physicochem Eng Asp. 1999;159:351–8. https://doi.org/10.1016/S0927-7757(99)00291-5.
57. Ahmat AM, Thiebault T, Guégan R. Phenolic acids interactions with clay minerals: a spotlight on the adsorption mechanisms of Gallic Acid onto montmorillonite. Appl Clay Sci. 2019;180:105188.
58. Chapman H d. (1965) Cation-Exchange Capacity. In: Methods of Soil Analysis. John Wiley & Sons, Ltd, pp 891–901

Publisher's Note Springer Nature remains neutral with regard to jurisdictional claims in published maps and institutional affiliations.

Springer Nature or its licensor (e.g. a society or other partner) holds exclusive rights to this article under a publishing agreement with the author(s) or other rightsholder(s); author self-archiving of the accepted manuscript version of this article is solely governed by the terms of such publishing agreement and applicable law.